Geotechnical Aspects of Underground Construction in Soft Ground – Ng, Huang & Liu (eds)
© 2009 Taylor & Francis Group, London, ISBN 978-0-415-48475-6

Monitoring and modelling of riverside large deep excavation-induced ground movements in clays

D.M. Zhang & H.W. Huang
Key Laboratory of Geotechnical and Underground Engineering of Ministry of Education, Tongji University, Shanghai, P.R. China
Department of Geotechnical Engineering, Tongji University, Shanghai, P.R. China

W.Y. Bao
China State Construction Engineering Corporation (SH), Shanghai, P.R. China

ABSTRACT: The Riverside large deep excavation of Shanghai international passenger center was 800 m long and 100–150 m wide with the depth of 13 m. The south long side of the deep excavation was at a distance of 4.6 m from the parallel flood wall of Huangpu River. The north long side was 5 m away from a historic building. Problems resulted from the large deep excavation was the asymmetric ground movements along the long sides due to the complex surrounding condition and surface surcharge. The monitoring during the excavation provided numerous data to study the characteristics of the ground movement and earth pressure. The numerical modelling was also adopted aim to predict the ground movements.

1 INTRODUCTION

The development of underground space along the bund of Huangpu River in Shanghai, China has resulted in excavations becoming progressively larger and closer to the River, where the groundwater table was just near the ground surface and a great number of underground works are within a few meters of the surface. The riverside excavations were all located close to the existing buildings, network and the city lifeline of flood wall. It has become a great challenge to protect these neighboring buildings and public utilities from damage during the deep excavation due to the complex geotechnical constraints and the small opening from the Huangpu River. The soils near the Huangpu River was usually weak with a very low strength and higher water content, which were a potential causes of the larger ground movement. Meanwhile, the complex and dense environments put forward a strict requirement on the ground movement controlling. It was difficult to determine the earth pressure acted on the retaining wall with any conventional earth pressure theory considering the small soil body left between retaining wall and flood wall. Besides, the retaining wall of riverside deep excavation was usually asymmetrically loaded with much higher earth pressure on one side, which was caused by great surface surcharge due to the existing buildings and the pile of the construction material. The stability of the deep excavation as a whole was worth considering to avoid any kinds of failure of the deep excavation and consequent damage on the environments.

However, there were few references for the construction of the large deep excavation because of the geotechnical condition and complex environment along the bund of Huangpu River. The deep excavation of Shanghai international passenger center (SIPC) was the largest and closest one to Huangpu River so far. The construction and the analysis method of the deep excavation of SIPC and the induced ground movement as well will be a useful and practical reference for the subsequent riverside large deep excavation.

2 PROJECT OUTLINE AND SOIL CONDITIONS

2.1 *Project outline*

The deep excavation of SIPC was 800 m long with the width of 100–150 m and the depth of 13 m. The large deep excavation was divided into two sub-excavations with the lengths of 480 m and 218 m respectively to reduce the risk of damage for the existing structure and the failure of deep excavation. The study presented in this paper was carried out based on the deep excavation with the length of 480 m. The sketch view of the project was illustrated in Figure 1. The space between the deep excavation and flood wall of Huangpu River was only

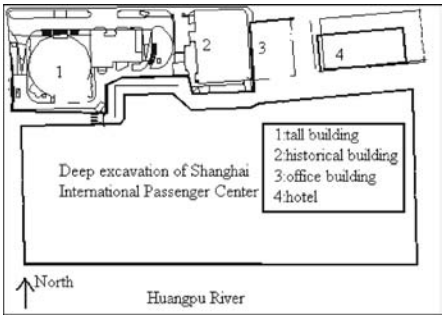

Figure 1. Sketch view of the project.

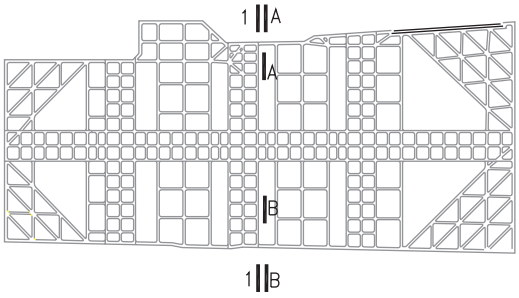

Figure 2. The plane view of strut arrangement.

4.6 m at south side. A number of existing buildings, including a historic building, were located along the north side of the deep excavation with a distance of about 5 m.

Bored piles supplemented by SMW piles wall were used as the retaining structure. The bored pile was 950 mm in diameter with a center-to-center space of 1150 mm. The effective length of the bored pile was 26 m and the embedment was adequate to provide sufficient passive earth pressure to keep the stability of the retaining wall. The SMW piles were 850 mm in diameter with an effective length of 20.8 m. The distance between SWM piles was 600 mm to guarantee the waterproof performance. The mix ratio of cement was as high as 20% for SMW piles. Three reinforced concrete struts were set at the depth of −0.9 m, −5.7 m and −9.6 m with the cross section of 1250 × 800 mm for the first strut and of 1200 × 800 mm for the second and third strut. The plane space of the strut was about 1.2 m and illustrated in Figure 2. The cross sections of the deep excavation were presented in Figure 3a and 3b.

The jet grouting belt of 4 m wide and about 4 m high was employed closely above the bottom of the deep excavation along the retaining wall. The grouting could significantly increase the capacity of the soil resistance for the retaining wall during the excavation. The bored pile was extended from 26 m to 27 m near

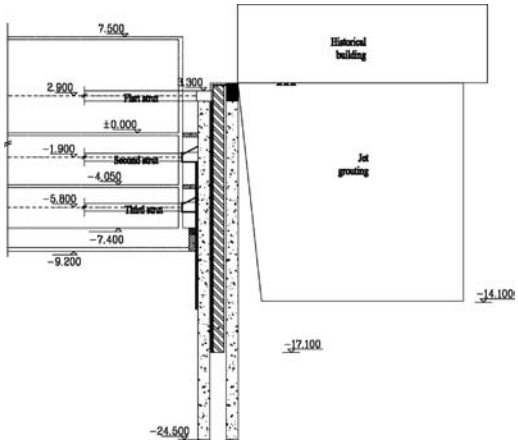

Figure 3a. A-A cross section of deep excavation.

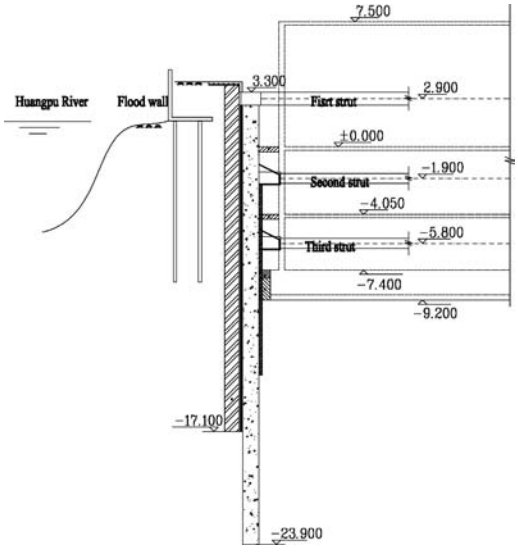

Figure 3b. B-B cross section of deep excavation.

the historic building to protect the building from crack and tilting. Besides, the isolation piles were specially designed to reduce to deep excavation-induced effect on the historic building.

2.2 *Soil conditions*

The soil profile throughout the deep excavation comprises the mixed filling to a depth of 6.4 m, which contains many obstacles and made a lot of trouble for the deep excavation, underlain by silt, silty clay and mucky clay. The retaining wall including the waterproof wall was embedded in the silty clay. The detailed characteristics of the soils were presented in Table 1.

Table 1. Soils characteristics throughout the deep excavation.

Soil	Depth m	Water content %	Bulk density kN/m^3	Compression modulus kPa	Cohesion kPa	Friction angle °
Mixed filling	6.38					
Silt	4.89	31.7	18.2	8170	8	28.5
Mucky clay with silt	4.96	40.5	17.5	4130	11	22
Mucky clay	7.17	49.7	16.6	2580	14	13
Silty clay 1	7.31	34.0	18.0	4570	17	17
Silty clay 2	4.05	33.3	17.8	8130	8	29
Silty clay 3	17.23	33.2	17.9	5240	17	23.5

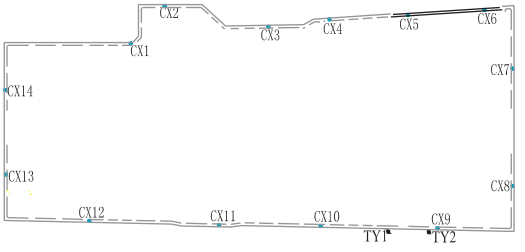

Figure 4. Monitoring layout of lateral displacements.

Table 2. Progress of excavation.

Date	corresponding excavation depth (m)
11/5/2005–11/11/2005	3
11/11/2005–12/2/2005	6.2
12/2/2005–1/3/2006	13
1/13/2006	completion of bottom plate

3 MONITORING OF EXCAVATION

As shown in Figure 4, 14 inclinometers, which were denoted by CX1 to CX14, were set into the retaining wall around the deep excavation. 2 earth pressure gauges denoted as TY1 and TY2 in Figure 4 were also installed close to the retaining wall to study the evolution of earth pressure of the small soil body between retaining wall and flood wall during excavation. The earth pressure gauges were installed every 5 m in the vertical overall 25 m.

The progress of excavation was presented in Table 2.

3.1 *Monitored lateral displacements*

Figures 5–8 showed the lateral displacements at monitoring points of CX1, CX3, CX12 and CX10 corresponding to the studied excavation stages. These inclinometers were close to the center of the long side

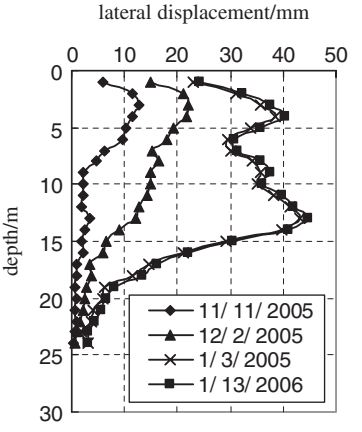

Figure 5. Lateral displacement at inclinometer CX1.

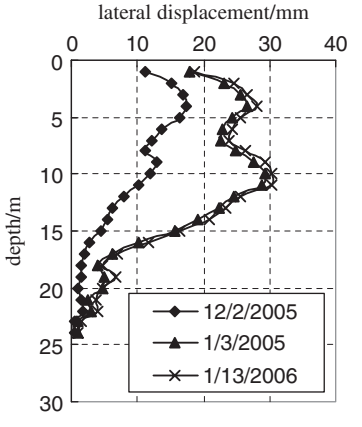

Figure 6. Lateral displacement at inclinometer CX12.

of the deep excavation and thus the readings were representative of the maximum displacement of the retaining wall. It could be found from figures 5–8 that the maximum lateral displacement was less than 60 mm during the whole excavation stage. Meanwhile,

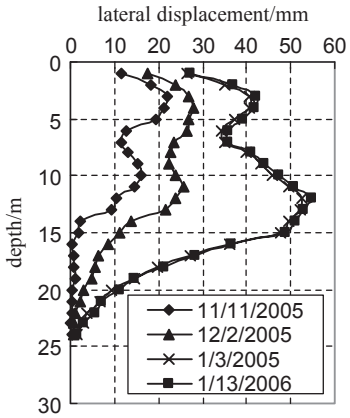

Figure 7. Lateral displacement at inclinometer CX3.

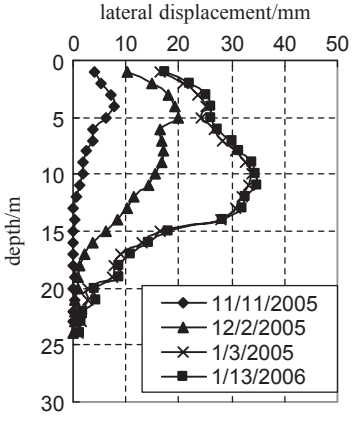

Figure 8. Lateral displacement at inclinometer CX10.

the lateral displacement exhibited asymmetric behavior along the two long sides of the deep excavation because of the following two reasons. Firstly, the earth pressure acted on the retaining piles was asymmetric because of the small soil body between Huangpu River and deep excavation. Secondly, the surface surcharge was asymmetric due to the existing buildings. Comparing the records of CX1 with CX12, CX3 with CX10, it could be found that lateral displacement of retaining wall was 15–29% smaller at the south side than north side. Unfortunately, the larger lateral displacement at north side would result in a potential damage to the neighboring historic building. Consequently, the jet grouting should be immediately carried out to improve the foundation of the historic building and it was proved to be an effective way to avoid the damage of crack and tilt of the building.

The recorded lateral movements at the top of retaining wall were presented in Figure 9. The five movement

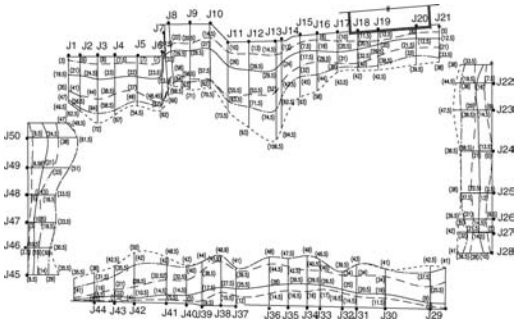

Figure 9. Distribution of lateral movement at the top of retaining wall.

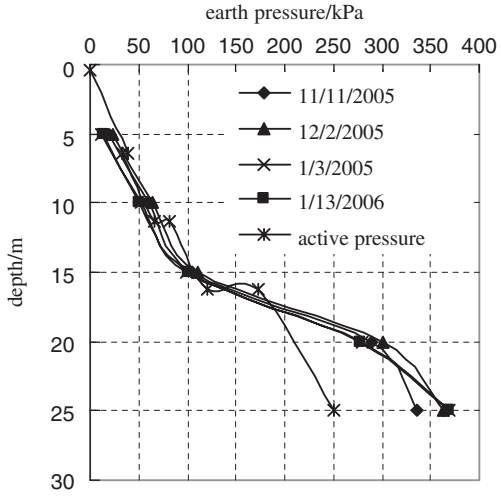

Figure 10a. Comparison of recorded earth pressure with calculated active earth pressure at TY1.

curves from outside to inside were corresponding to the excavation depth of 2.3 m, 6.2 m, 13 m, completion of bottom plate and completion of underground structure respectively. The maximum lateral movement at the top of retaining wall reached 106.5 mm at the north side, while it was only 50 mm at the south side, when the underground structure was completed. These phenomena also confirmed the influence of asymmetric earth pressure on the movement of the retaining wall.

3.2 *Evolution of earth pressure*

The monitored earth pressure was illustrated in Figure 10a and 10b with calculated one. The calculated active earth pressure was obtained using Rankine earth pressure theory.

From figure 10a and figure 10b, it could be found that the monitored earth pressure at top 15 m was very

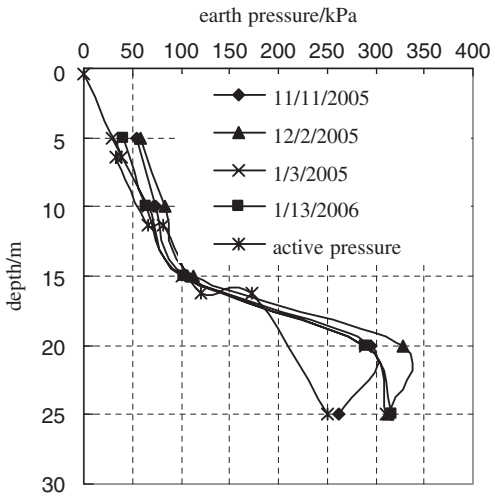

Figure 10b. Comparison of recorded earth pressure with calculated active earth pressure at TY1.

close to the active pressure for both monitored points. It became much larger than active pressure below 15 m. Two factors could be contributed to the distribution of the earth pressure. One was that the magnitude of lateral displacement of the retaining wall was larger in the top 15 m than that of below 15 m, and it could be verified from Figures 5–8. The other cause was that the small bulk of the soil body against the retaining wall at top 15 m. It could be found from Figure 3 that the soil body in the top 15 m was much smaller than in below 15 m. Both figure 10a and figure 10b implied that the soil body had a significant effect on the distribution of earth pressure against the retaining wall.

However, the earth pressure at north side of the deep excavation was not monitored. No comparison could be performed between the two sides.

4 MODELLING OF DEEP EXCAVATION

2-D numerical modelling was carried out using FEM code of Plaxis v8 considering the narrow plane characteristic of the deep excavation. The cross section 1–1 shown in Figure 2 was adopted in FEM analysis because it was almost the center of the deep excavation and near the historic building as well.

4.1 *Numerical model*

The overall width of deep exaction at cross section 1–1 was 100 m with excavation depth of 13 m. The width of the numerical model was 240 m, which was 18 times as wide as the depth of the excavation. The vertical dimension was 50 m, which was more than 3.5 times the depth of the excavation. The model dimension was

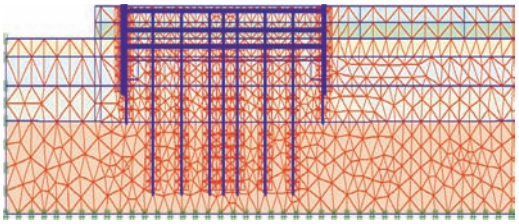

Figure 11. The FEM mesh.

Table 3. Parameters of retaining piles and ground improvement.

	Elastic modulus kPa	Poison's ratio
Retaining piles	3.3×10^7	0.15
Strut	3.0×10^7	0.15
Ground improvement	1.4×10^5	0.20

large enough to lower the boundary effect. A linear elastic model was adopted for the ground improvement. The retaining wall as well as the strut was simplified as elastic beam in numerical modelling. The soils were simulated with Mohr-coulomb model. The numerical simulation was performed with 15-node isoparametric finite elements under the assumption of plane strain conditions. The FEM model was presented in Figure 11.

The boundary conditions in the numerical simulation contain the following two types, one was the displacement boundary condition, and the other was the drainage condition. A free displacement boundary condition was adopted at the ground surface. It was assumed that no horizontal nor vertical displacement taken place at the lower boundary, for it was beyond the influence of deep excavation. The lateral displacements at left – and right – hand boundary were both fixed as zero. The drainage condition at the ground surface was assumed to be free, hence the excess pore pressure was kept as zero along the ground surface; meanwhile the lower boundary as well as the left – and right – hand boundary condition were considered to be kept as hydrostatic pore pressure during excavation. The initial effective stresses and hydrostatic pore pressure were calculated based on the weight of the soil and the underground water condition.

4.2 *Parameters used in numerical modelling*

The parameters of retaining structure and ground improvement used in the numerical analysis were listed in Table 3. The soil parameters could be referenced as Table 1. The interface between retaining piles and soil was adopted and the interface parameters were determined according to Plaxis manual. The modulus

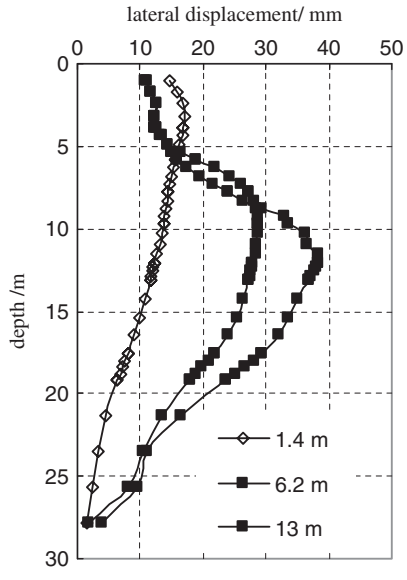

Figure 12. Evolution of lateral displacements at south side of deep excavation.

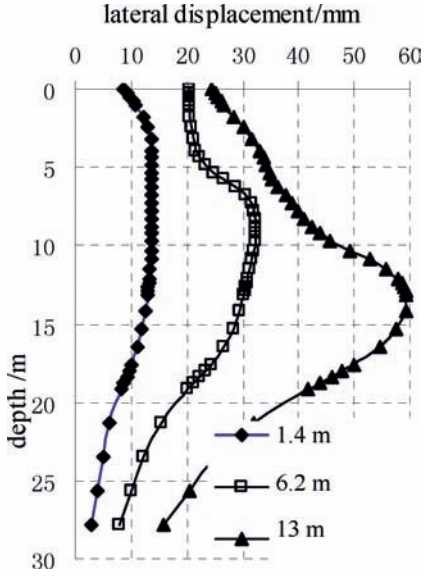

Figure 13. Evolution of lateral displacements at north side of deep excavation.

of resilience was adopted for soils. The modulus of resilience was obtained by back-analyzing the monitored lateral displacements of the first excavation progress shown in Table 2. It was found that the modulus of resilience was as 5 times high as the compression modulus for soils.

4.3 *Numerical modelling procedure*

The excavation was modeled with 7 consecutive steps shown as following: STEP 1 was to determine the initial stress state due to the gravity of soils. STEP 2 was used to exert the loading of existing buildings on the surface with the magnitude of 60–70 kPa according to the type of the buildings. The movements induced in STEP 1 and 2 were reset to zero in the modelling. STEP 3 represented the construction of retaining wall and ground improvement, the surcharge of 20 kPa was also loaded at this step. STEP 4 meant the first excavation to 1.4 m deep and the construction of first strut. In STEP 5, the second strut was set after excavating to 6.2 m deep. Excavating to 10 m deep and the third strut was finished in STEP 6. The excavation was completed and bottom plate was constructed in STEP 7. Dewatering was considered during the excavation by changing water table.

4.4 *Calculated lateral displacements*

Figures 12–13 presented the evolution of lateral displacements with excavation progress. The lateral displacements of south side of the retaining piles reached 28.8 mm, 38.4 mm respectively when excavated to the depth of 6.2 m and 13 m. They were smaller than those of north side of the retaining wall, which were 32 mm and 60 mm. It could be found that the maximum lateral displacement at north side was 1.5 times larger than that of south side of the retaining wall by comparing figure 12 and figure 13.

The comparison between calculated and monitored lateral displacement could be carried out because cross section 1–1 was coordinate with inclinometer CX3 and CX10. The monitored lateral displacements were 57.8 mm and 35 mm at monitored points CX3 and CX10 corresponding to the excavation depth of 13 m, while the accordingly calculated ones were 60 mm and 38.4 mm respectively. The agreement between calculation and monitoring implied the validation of the simulation procedure of FEM modelling with back-analysis on the modulus of resilience of soils. Besides, the consideration of main influential facts, such as surface surcharge due to existing loading and piling of construction material, the process of excavation, the supplemented techniques of dewatering and ground improvement, was essential in the FEM modelling to reasonably predict the behavior of the retaining piles.

5 CONCLUSIONS

The lateral displacement of Riverside deep excavation with complex surrounding environment was studied with monitoring data and FEM modelling. The lateral displacements of the retaining wall were asymmetric because of the asymmetric earth pressure. The maximum lateral displacement at north side was almost 1.5

times as large as that of south side of the deep excavation. The earth pressure was close to the active earth pressure in top 15 m due to the large lateral displacement and small soil body against the retaining wall. The earth pressure was much larger than active pressure below 15 m. It was found the soil body bulk had a noticeable effect on the distribution of earth pressure against retaining wall.

REFERENCES

Chang, C. T. & Sun, C. W. et al. 2001. Response of a Taipei rapid transit system TRTS tunnel to adjacent excavation. *Tunnelling and Underground Space Technology* 16: 151–158.

Yamagushi, I. & Yamazaki, I. et al. 1998. Study of ground – tunnel interactions of four shield tunnels driven in close proximity, in relation to design and construction of parallel shield tunnels. *Tunnelling and Underground Space Technology* 13(3): 289–304.

Zhang, D. M. & Huang, H. W. 2007. Ground movements and controlling measurements in deep excavation under asymmetric loading. *Proceeding of 10th national conference on soil mechanics. Chongqing, 1–4 Novermber 2007 (in press).* (in Chinese).